Proceeding of the IEEE
International Conference on Robotics and Biomimetics
Dali, China, December 2019

Design and Safety Control of a High-Payload Nursing Robotic Arm with Tactile Skin

Jiahao Wu, Yanshu Song, Hailin Huang, Fei Liu, Junan Chen and Bing Li*

Abstract— **Service robots are being increasingly used to replace human beings in carrying out various sophisticated, heavy and even dangerous tasks. In order to solve the problem of labor shortage in the medical and nursing industry, this paper proposes a novel high-payload robotic arm for nursing tasks, which can help caregivers to lift and transfer patients. Firstly, we simulate and analyze the specific nursing tasks and application scenarios, and determine its kinematics configuration and load capacity parameters of each joint. Then we design and fabricate the modular and low flexibility robotic joints for the prototype. To avoid the occurrence of safety accidents while lifting patients, we design a new kind of tactile skin based on the resistance characteristic of varistor materials, using which a safety control algorithm is proposed. Experiments show that it can meet the requirements of load capacity and position control accuracy, and the proposed safety control method can effectively avoid many dangerous situations.**

I. Introduction

The development of robotics technology and the shortage of labor force have resulted in a large number of assistive robots of various types. For example, Christian [1] proposed an intelligent wheelchair robot which combined a noninvasive EEG-based human-robot interface and an autonomous navigation system to help severely disabled people who cannot steer a wheelchair. Ionut Mihai designed a biped robot called SHERPA [2], which has multiple 2-DOF (degree of freedom) cable-driven differential modular joints and can deliver goods by walking. Wing [3] presented a novel rescue robot system called RescueBot. It consists of a crawler-type robotic chassis and a wearable suit which allows the RescueBot replace rescue workers in performing different types of rescue tasks.

Assistive robots for nursing tasks are emerging to address the social need due to the changing demographic trends such as an ageing population. Barrett company [4] developed a cable-driven robot called WAM, which has six joints based on differential mechanisms and can be used to assist in the treatment of stroke. Ming [5] designed a feeding assistive robot consisting of four modular flexible joints, which could meet the needs of people with upper limb disabilities or dysfunctions in gaining independence in eating. Liu [6] developed a cable-driven serial-parallel manipulator which has a large load/mass ratio and high payload capcity, and it is expected to be applied in the context of helping the elderly and disabled. Greg [7] presented an assistive robot to undertake dressing tasks using a compliant robotic arm on a mannequin and several strategies are explored on how to undertake this task with minimal complexity and a mix of sensors.

Service robots used to perform nursing tasks need to have direct contact with humans in uncertain environments, which brings great security challenges. Therefore, researches on the safety mechanisms, safety sensors and safety control methods of nursing robot have been wildly carried out to prevent accidents. Mukai et al developed the RIBA nursing robot [8] with differential modular robotic joints which can generate greater output torque at the same joint sizes [9]. To ensure the safety of human-robot interaction, the soft materials such as polyurethane foam and tactile sensors are wrapped on the robotic arms for tactile guidance, and adopt distance adjustment between both arms to fit the lifted patient [10]. The RONA nursing mobile robot [11] developed by Hstar Technologies is a physical assistance system that works effectively in a hospital environment under telepresence control by nurses or physicians. It has a humanoid design with bimanual dexterous manipulators employing a series-elastic-actuation (SEA) system, which can provide the manipulators compliance, safety, and the strength to lift patients weighing up to 300lbs. Waseda University proposed the human symbiotic robot TWENDY-ONE [12], which can provide physical supports to the elderly such as attendant care with high-power and kitchen supports with dexterity. The whole body of the manipulator is covered with flexible silicone materials and distribution pressure sensors ensuring that the robot can be stopped in time when dangerous situations occur.

In view of the shortage of medical staff in hospitals, this paper proposes a novel high-payload nursing robotic arm which can be used to assist nurses in moving patients between stretchers and beds. To ensure safety, we design a new kind of tactile robotic skin based on the resistance characteristic of varistor materials, and propose a safety control method based on it. Experiments have verified that the manipulator and the tactile skin can meet requirements of load capacity for nursing tasks and accuracy of pressure measurement, respectively. The proposed safety control algorithm can also effectively avoid the occurrence of dangerous situations in the process of man-machine interaction.

The remainder of this paper is organized as follows. Section II and III introduce the design and manufacture of the high-payload robotic arm and the soft tactile skin, respectively. Section IV describes the proposed safety control method to

This work was supported by the National Key Research and Development Program of China (Grant No. 2017YFB1302200), and in part by the Key Research and Development Program of Guangdong Province, China (Grant No. 2019B090915001).

Jiahao Wu, Yanshu Song, Hailin Huang and Fei Liu is with School of Mechanical Engineering and Technology, Harbin Institute of Technology, Shenzhen 518055, China.

Junan Chen is with the School of Electronic and Information Engineering, Harbin Institute of Technology, Shenzhen 518055, China.

Bing Li is with State Key Laboratory of Robotics and System, Harbin Institute of Technology, Harbin 150001, China and with School of Mechanical Engineering and Technology, Harbin Institute of Technology, Shenzhen 518055, China. (Corresponding author, e-mail: libing.sgs@hit.edu.cn).

978-1-7281-6321-5/19//$31.00 ©2019 IEEE

avoid the occurrence of dangerous situations in nursing process. Three groups of experiments were conducted and the analysis of results is presented in Section V. Finally, Section VI concludes this paper.

II. Mechanical Design

A. Requirement analysis

The robotic arm is mainly used in hospitals and nursing rooms to lift and transfer patients. Considering the complexity of the working environment and the requirement of adapting patients' postures, we determine the DOF of the manipulator arm to be 6. The joints placements are designed referring to the human arm, as depicted in Fig. 1. The *Sho1-3* are imitating the shoulder joints, and are followed by the two elbow joints *Elb1-2* and the Wrist joint.

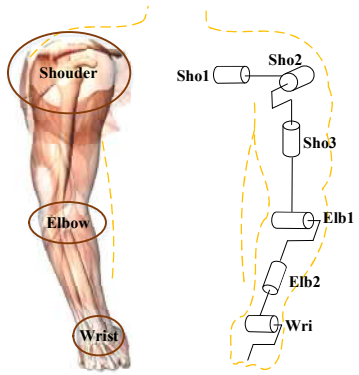

Fig. 1. Diagram of robotic arm's joints placements.

This nursing robotic arm is used to carry out the task of lifting and moving patients, so the basis of ensuring its safety is that the selected motors, reducers and other components can meet the strength requirements. We build a dynamic simulation model to obtain the maximum load torque of joint. The actual load on single arm is less than 50kg because patients generally weigh less than 100kg. In addition, only the *Sho1-3* and *Elb1* joints need to bear large torque, so we analyze the demand of output torque of these four joints. In order to enable the manipulator arm to complete nursing tasks in various environments, we set simulation constraint parameters according to the most extreme conditions. As shown in Fig. 2, the length of the upper arm is 500mm and its quality is 15kg, the length of the lower arm is 500mm and its quality is 10kg, and finally the block pressed on the center of the lower arm is 50kg.

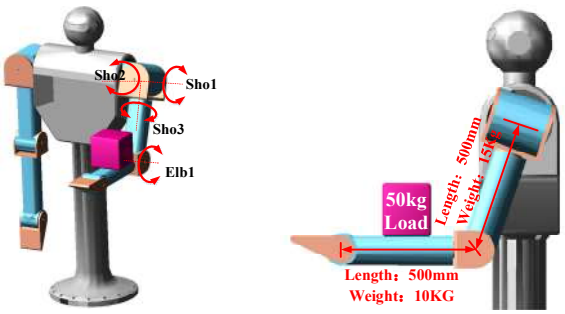

(a) Model joints placements. (b) Model constraint parameters.

Fig. 2. Dynamic simulation model.

When the manipulator lifts the load with different postures and accelerations in the simulation environment, the maximum output torques and rotation angle ranges of the Sho1-3 and Elb1 are shown in Table 1.

TABLE I
DESIGN PARAMETERS OF THE Sho1-3 AND Elb1 JOINTS

Joint	Maximum output torque (Nm)	Rotation angle range (degree)
Sho1	471.2	-90-90
Sho2	252.1	0-90
Sho3	124.6	-90-90
Elb1	147.3	-90-90

B. Mechanical structure

The upper arm consists of four joints (*Sho1-3* and *Elb1*), as shown in Fig. 3. The *Sho1-2* adopt the traditional joint module, selecting the suitable DC brushless motor, harmonic reducer and servo driver according to the design parameters, and installing them sequentially. Compared with other types of reducers, harmonic reducer has the advantages of large deceleration ratio and strong load-carrying capacity, but it also brings greater flexibility and lower positional accuracy to the robotic joint, so high-precision magnetic grating encoders are equipped at the motor side and the output side of the harmonic reducer to improve the accuracy position control. In addition, we design a frictional brake at the end of each motor, so that the robot can hold the patients stably and safety in the event of a power failure. Test results show that the maximum output torque of joints *Sho1-2* are 521Nm and 320Nm, respectively.

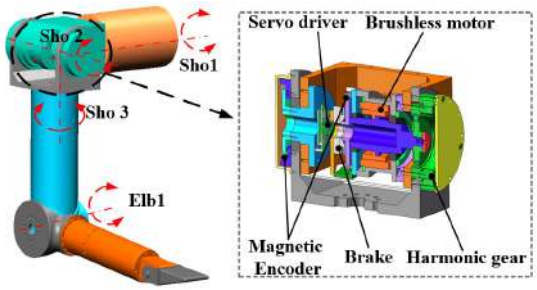

Fig. 3. The structure of *Sho1-2* joints.

In order to obtain high torque density and improve space utilization, Joint *Sho3* and *Elb1* are arranged symmetrically in reverse direction in the same upper arm shell. At the same time, we design a multi-stage deceleration mechanism for each joint to improve its output torque. As shown in Fig. 4, the brushless DC motors (Maxon EC 52) are staggered on the shell. The motor of *Sho3* is connected to a planetary reducer to achieve the first stage decelerationand then connected to a pair of spur gears to achieve the second stage deceleration. Finally, it is connected to a hollow harmonic reducer to realize the third stage deceleration and output torque and motion. Similarly, the motor of *Elb1* achieves the first stage deceleration through a planetary reducer, and changes its direction by a pair of bevel gears, and finally is connected to a harmonic reducer to achieve a larger torque output. In order to avoid the influence of backlash in gear transmission on the accuracy of position control, we also design high-precision encoders both at motor sides and output sides of

the two joints. And the *Elb1* joint is equipped with frictional brake to ensure safety. According to the experimental measurements, the maximum output torque is 147Nm (*Sho3*) and 155Nm (*Elb1*), respectively. The cross section (*Sho3* and *Elb1*) are shown in Fig. 4.

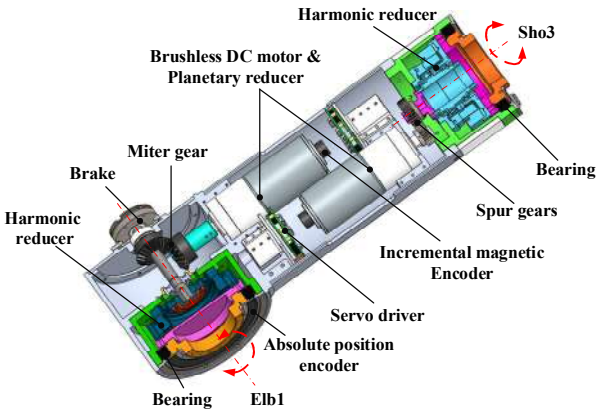

Fig. 4. The cross section of the *Sho3* and *Elb1 joints.*

The cross section of the lower arm is shown in Fig. 5, which consists of the joint *Elb2* and the joint *Wri*. In joint *Elb2*, the brushless motor is directly connected with a harmonic reducer to achieve single-stage deceleration and output motion. For joint Wri, the motor achieves the first stage deceleration through a planetary reducer, and then it is connected to a right-angle reducer to realize the second stage deceleration and the change of the rotation direction. Each joint of the manipulator arm adopts hollow design form to ensure that the cable can be completely wrapped in the interior of the robot.

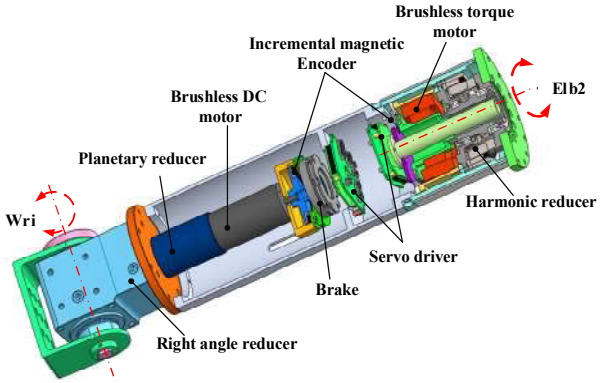

Fig. 5. The cross section of the lower arm.

III. TACTILE SKIN DESIGN

A. Sensing principle

In order to detect the pressure and its position acting on the manipulator, we design a novel kind of flexible robotic skin which has tactile function. Its core component is the membrane-structured matrix of piezoresistive flexible film sensors produced by transferring nano-sensitive materials and silver paste to flexible film substrates through a precise printing process, and the resistance of sensor unit decreases with the increase of pressure. Each sensor matrix consists of 8 × 8 detection units, which forms a square with a side length of 125 mm. The specific feature parameters are shown in Table II.

TABLE II
SPECIFIC FEATURE PARAMETERS OF THE ROBOTIC SKIN

Feature	Parameter
Range of resistance	1-200MΩ
Measuring range	0-5kg (each unit)
Thinckness	<0.5mm
Weight	<5g
Working range	0-5kg (each unit)
Working voltage	3-5V
Working temperature	-50-95℃

To protect the resistive pressure elements from damage, we embed them in pieces of 7mm thick skin substrates which are processed from skin-friendly photosensitive resin Nitrile Butadiene Rubber (NBR) and used as buffers between the patient and the rigid robotic arm. NBR is selected because of its chemical stability, suitable elasticity, and ease of manufacture, making the tactile skin be able to attach to any curved surface.

As shown in Fig. 6, this tactile skin is wrapped around the manipulator, which not only enables the manipulator to perceive the pressure from various positions, but also provides a more comfortable experience [13] when contacting with patients. In order to avoid the problem of signal interference caused by a large amount of interlaced wires, we equip every two pieces of tactile skin with one tactile sensor acquisition board. Based on the piezoresistive characteristics of pressure sensor unit, it can collect current signals of 64×2 units by scanning multiplexer circuit, and convert them into digital signals through A/D converter circuit, and the highest acquisition frequency is 250Hz.

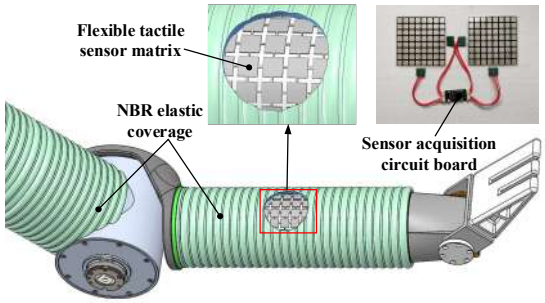

Fig. 6. The structure of the tactile skin and its placement positions.

B. Sensing calibration

We design an experiment to calibrate the tactile sensors, and to obtain the mathematical relationship between the force and the voltage according to the Ohm's law. As shown in Fig. 7(a), the applied pressure values are measured by high-precision digital pressure sensor, and the corresponding resistance values of pressure sensor units are measured by a multi-meter. The mathematical relationship between the resistance of the pressure sensor unit and the pressure is shown in Fig. 7(b). It can be seen that the resistance decreases with the increase of the pressure, while the relationship between conductivity and pressure is very linear. We get the numerical relationship between them by least-squares method, as shown in (1).

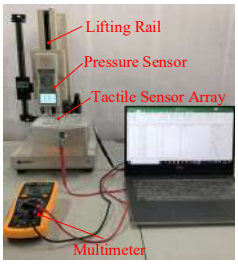

(a) Sensing calibration platform.

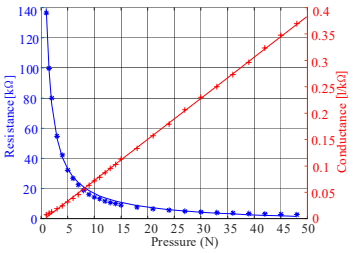

(b) The actual relationship between resistance and pressure.

Fig. 7. Sensing calibration process.

$$F_{ij} = 125.3 \times R_{ij}^{-0.963} \quad i, j \in [1, 2, 3 \cdots, 8] \tag{1}$$

Where F_{ij} is the force detected by the pressure sensor unit in the i-th row and the j-th column of the tactile skin, and R_{ij} denotes the corresponding resistance.

IV. Safety Control System

A. Control system design

As shown in Fig. 8, the control system of the robotic arm is mainly composed of three parts: main controller, joint module and tactile module, and each module communicates via CAN bus. The main controller is designed based on the Robot Operating System (ROS). Each joint module is equipped with an independent servo driver, which receives position commands through the 402 protocol of CAN-open and communicates with the main controller through USB to CAN. Similarly, the current tactile signals in 10 pieces of tactile sensor matrix are collected and processed into pressure signals through five acquisition boards, and then transmitted to the main control board through CAN bus. The main controller receives the pressure information on each tactile skin, and then makes decisions based on our proposed security algorithm, and finally sends motor motion control instructions to each servo driver.

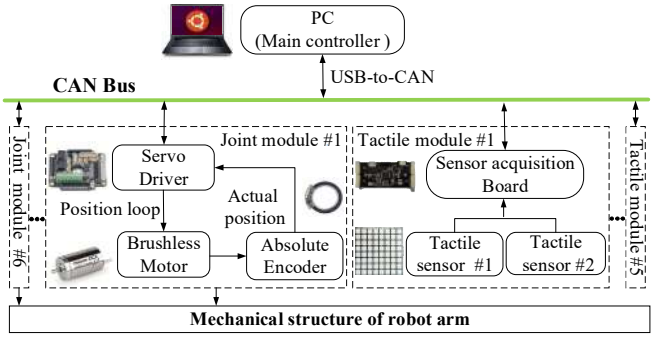

Fig. 8. The control system of the robot arm.

B. Safety control method

Due to the limitation of the physical structure of the manipulator and the uncertainty of the patient's postures, the following dangerous situations may occur during the process of lifting and transferring the patient (Fig. 9):

(a) During the process of lifting a patient, the patient's center of gravity is too far ahead of the manipulator arm.

(b) During the process of transferring a patient, the patient's center of gravity is too biased towards one of the double arms.

(c)The patient's weight exceeds the payload of the manipulator arm.

These situations can overload the manipulator arm and even cause the patient to fall off from the arm, which are major safety accidents. Therefore, it is necessary to develop a safety control strategy to ensure the safety of the patient.

(a) Too far ahead of the arm. (b) Too biased towards one side. (c) Weight exceeds the payload.

Fig. 9. Dangerous situations while lifting and transferring the patient.

As shown in Fig. 10 (a), during the process of transferring a patient, the tactile skin can be used to detect the relative position and contact force between the patient and the robotic arm, and the ideal patient's center of gravity was set to the center of the arm. As shown in Fig. 10 (b), the manipulator arm has three types of postures when contacting with patients, i.e. the initial pose, the contact pose, the lift pose. In order to prevent the occurrence of the above dangerous situations, we propose a safety control method which can imitate the human mind and make motion decisions.

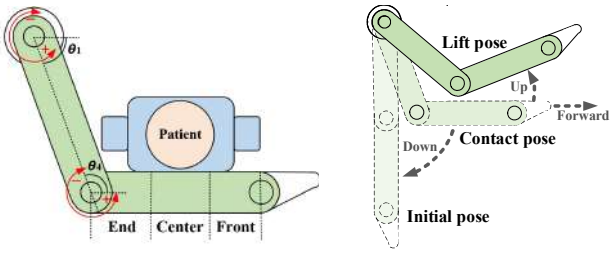

(a) The correct contact situation. (b) The three types of postures.

Fig. 10. Postures of the robotic arm in task execution.

Firstly, when the manipulator is in contact with the patient, the tactile skin on the arm can sense pressure size and distribution. So the patient's gravity and real-time gravity center position can be calculated by (2) and (3).

$$G_L = \sum F_{ij} \tag{2}$$

$$P_L = \frac{\sum F_{ij} \bullet P_{ij}}{F_L} = \frac{\sum 125.3 \times R_{ij}^{-0.963} \times P_{ij}}{F_L} \tag{3}$$

Where F_{ij} is the force detected by the pressure sensor unit in the i-th row and the j-th column of the tactile skin, G_L is gravity of the patient, P_{ij} is the position vector of the corresponding unit,

and P_L denotes the position of the center of gravity of the patient.

After the gravity and the position of the center of gravity are detected, the main control board will indicate the movement of each joint according to the following rules:

(1) In the process of lifting a patient: if it is detected that the load of each arm is greater than 50 kg, the arm will slowly put the patient down and sound an alarm.

(2) After touching the patient: if it is detected that the patient's center of gravity is in the first third of the lower arm, the arm will be slowly put down and stretch forward until the patient's center of gravity is adjusted in the middle of the arm.

(3) After the arm posture adjustment is completed: if the patient's weight and contact position meet the safe lifting requirements, the robotic arm will move to the lift pose according to the pre-planned trajectory

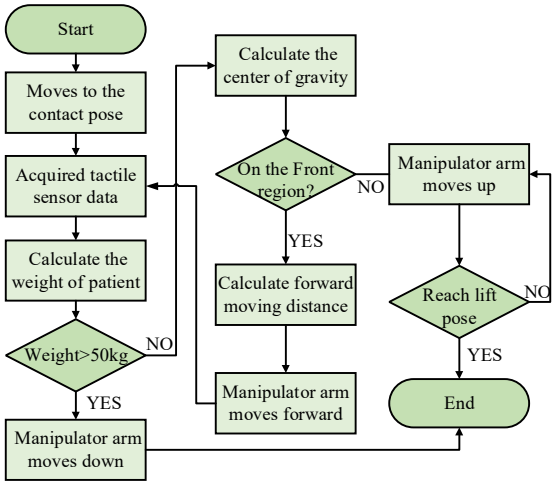

Fig. 11. The flow chart of the safety control method.

The flow chart of this safety control method is shown in Fig. 11. Using the control strategies can ensure that the patient does not slip or fall from the robotic arm during the lifting and transferring processes, thereby ensuring the safety when the manipulator arm carrying out the nursing task.

V. Experiments And Results

A. Load capability

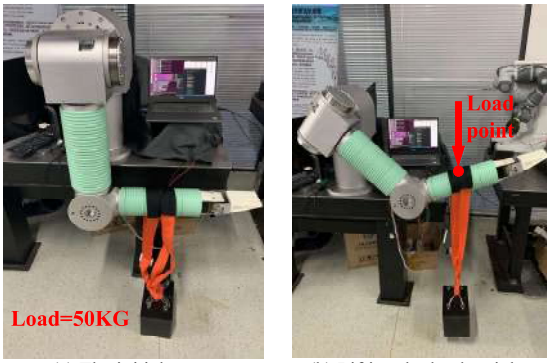

(a) The initial state. (b) Lifting the load weight.

Fig. 12. The load capability test platform.

This manipulator arm needs to be able to carry the weight of a patient when performing nursing tasks, according to design requirements, the single arm actual payload is 50kg. As shown in Fig. 12, we fix the manipulator on a stationary vibration isolation platform, and hang a 50kg load on the middle of the lower arm with nylon rope. It can be seen that the manipulator arm can follow the pre-planned path, and lift the weight smoothly, so it can meet the design requirements.

B. Tactile skin performance

To test the perception performance of the proposed tactile skin, we connect two pieces of the tactile skin on the foam board and place a weight of 10 kg on them as shown in Fig. 13 (a). The Fig. 13 (b) shows the pressures measured by each pressure sensing, and the highest prism represents the calculated center of gravity of the load. It can be seen that the pressure distribution measured is consistent with the actual situation. The total gravity measured ranges from 9.92kg to 10.35kg, so the difference in measurements by the tactile sensor is less than 5%. The results show that the tactile skin has high resolution and measurement accuracy, which can meet the requirements of safe contact detection.

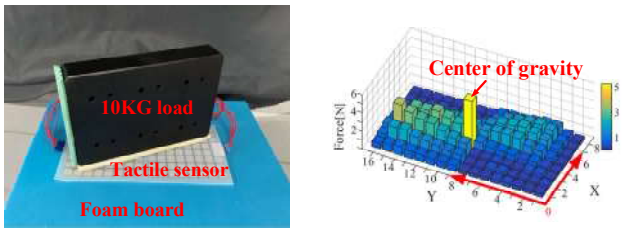

(a) The test platform. (b) The pressure measurement results.

Fig. 13. Tactile skin performance test.

C. Safety control

In order to verify the proposed safety algorithm based on tactile skin, we press the different areas of the manipulator arm to simulate the patient's contact with it. The specific experimental process is as follow:

(1) Firstly, the manipulator moves from the initial position shown in Fig. 14 (a) to the posture shown in Fig. 14 (b) to prepare to lift the patient.

(2) Then pressing the front side of the lower arm, the pressure distribution perceived by the tactile skin is shown in Fig. 15 (a), the total pressure is 21.6kg, less than 50kg. Then, the main control board processes this pressure distribution information and gets that the center of gravity of the load is in the first third of the arm, so the arm automatically adjusts its posture forward as shown in Fig. 14 (c).

(3) Finally, pressing the middle of the lower arm with force less than 50 kg after the manipulator adjusts its posture. The pressure distribution perceived by tactile skin is shown in Fig. 15 (b), and total pressure is 22.3kg. The main controller processes this pressure information and concludes that the load weight and the position of action point are both meet the safe lifting requirements, so it performs the action of lifting the patient up as shown in Fig. 14 (d).

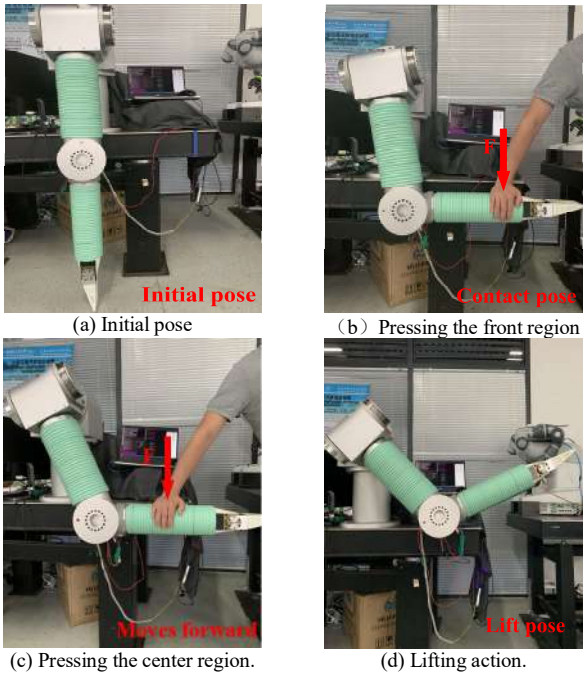

(a) Initial pose (b) Pressing the front region

(c) Pressing the center region. (d) Lifting action.

Fig. 14. The experimental process of safety control.

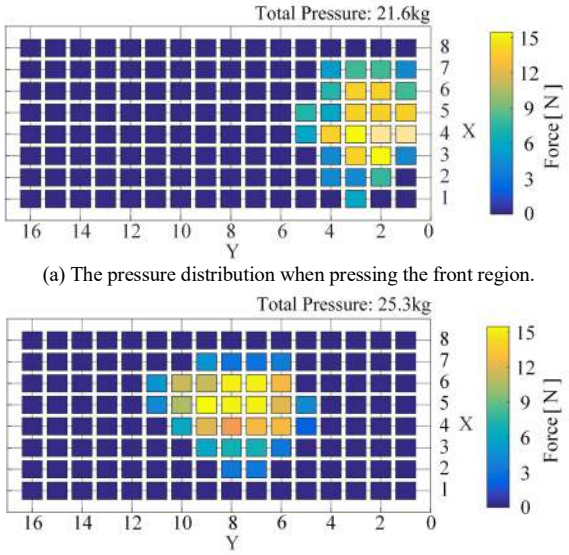

(a) The pressure distribution when pressing the front region.

(b) The pressure distribution when pressing the center region.

Fig. 15. The pressure distribution perceived by the tactile skin.

The result shows the pressure distribution information measured by the tactile skin can be used to guide the robotic arm to make appropriate movement according to the proposed safety control method. Compared with traditional visual-based methods, the tactile-based motion adjustment method will not be affected by complex unstructured nursing environment. So it can realize the higher stability and safety in nursing tasks.

VI. Conclusion

In this paper, we design a novel high-payload manipulator for nursing tasks. In order to ensure the safety of the manipulator contacting with patients, we design a new kind of robotic skin with tactile perception function and propose a safety control system. Experiments show that our manipulator can meet the requirement of carrying capacity, and the designed tactile robotic skin can measure the pressure distribution accurately. Finally, our safety control system can effectively avoid the occurrence of some dangerous situations. The tactile skin and the safety control strategy proposed in this paper will help to improve the comfort and safety in the process of human-machine interaction. However, there are still some problems, such as the inconsistencies in resistance characteristics, and the invalidation of the tactile skin edges. Further work will focus on solving these problems and making it more general, and based on it to improve safety control method to adapt different types of nursing task.

References

[1] C. Mandel, T. Lüth, T. Laue, T. Röfer, A. Gräser and B.Krieg-Brückner, "Navigating a smart wheelchair with a brain-computer interface interpreting steady-state visual evoked potentials," *2009 IEEE/RSJ International Conference on Intelligent Robots and Systems*, St. Louis, MO, 2009, pp. 1118-1125.

[2] I. M. C. Olaru, S. Krut and F. Pierrot, "Novel mechanical design of biped robot SHERPA using 2 DOF cable differential modular joints," 2009 IEEE/RSJ International Conference on Intelligent Robots and Systems, St. Louis, MO, 2009, pp. 4463-4468.

[3] W. K. Chung, Y. Yang, N. Cui, H. Qian and Y. Xu, "Design of a rescue robot with a wearable suit augmenting high payloads rescue missions," *2017 2nd International Conference on Advanced Robotics and Mechatronics* (ICARM), Hefei, 2017, pp. 704-711.

[4] Ian Sharp, James Patton, Molly Listenberger, and Emily Case. Haptic/graphic rehabilitation, "Integrating a robot into a virtual environment library and applying it to stroke therapy," *Journal of Visualized Experiments*: JoVE, (54), 2011.

[5] M. Guo, P. Shi and H. Yu, "Development a feeding assistive robot for eating assist," *2017 2nd Asia-Pacific Con-ference on Intelligent Robot Systems* (ACIRS), Wuhan, 2017, pp. 299-304.

[6] F. Liu, W. Xu, H. Huang, Y.Ning, and B. Li, "Design and Analysis of a High-Payload Manipulator Based on a Cable-Driven Serial-Parallel Mechanism," *Journal of Mechanisms and Robotics*. October 2019; 11(5): 051006.

[7] G. Chance, A. Camilleri, B. Winstone, P. Caleb-Solly and S. Dogramadzi, "An assistive robot to support dressing - strategies for planning and error handling," *2016 6th IEEE International Conference on Biomedical Robotics and Biomechatronics (BioRob)*, Singapore, 2016, pp. 774-780.

[8] T. Mukai et al., "Development of a nursing-care assistant robot RIBA that can lift a human in its arms," *2010 IEEE/RSJ International Conference on Intelligent Robots and Systems,* Taipei, 2010, pp. 5996-6001.

[9] K. Wang, H. Qian, Y. Yang and Y. Xu, "A novel Differential Modular Robot Joint — Design and implementation," 2013 IEEE International Conference on Robotics and Biomimetics (ROBIO), Shenzhen, 2013, pp. 2049-2054.

[10] T. Mukai et al, "Tactile-based motion adjustment for the nursing-care assistant robot RIBA," *2011 IEEE International Conference on Robotics and Automation,* Shanghai, 2011, pp. 5435-5441.

[11] J. Hu et al., "An advanced medical robotic system augmenting healthcare capabilities - robotic nursing assistant," *2011 IEEE International Conference on Robotics and Automation*, Shanghai, 2011, pp. 6264-6269.

[12] H. Iwata and S. Sugano, "Design of human symbiotic robot TWENDY-ONE," *2009 IEEE International Conference on Robotics and Automation,* Kobe, 2009, pp. 580-586.

[13] Y. Ohmura, Y. Kuniyoshi, and A. Nagakubo, "Conformable and scalable tactile sensor skin for curved surfaces," *in Proceedings 2006 IEEE International Conference on Robotics and Automation*, 2006. ICRA 2006. IEEE, 2006, pp. 1348–1353.